ELSEVIER

Ceramics International 25 (1999) 639–648

CERAMICS INTERNATIONAL

Structure–electrical properties relationships in TiO_2-doped stabilized tetragonal zirconia ceramics

F. Capel [a], C. Moure [a], P. Durán [a,*], A.R. González-Elipe [b], A. Caballero [b]

[a] *Instituto de Cerámica y Vidrio (CSIC), Departamento de Electrocerámica, 28500-Arganda del Rey, Madrid, Spain*
[b] *Instituto de Ciencia de Materiales de Sevilla (CSIC-University de Sevilla) y Dto. de Química Inorgánica, Centro de Investigaciones Científicas "Isla de la Cartuja", Avda. América Vespucio s/n, 41092 Seville, Spain*

Received 5 May 1998; received in revised form 8 June 1998; accepted 7 August 1998

Abstract

The tetragonal zirconia solid solution field in the ternary system ZrO_2–Y_2O_3–TiO_2 has been established, and the influence of TiO_2 addition on the electrical properties of the formed ternary Ti-YTZP solid solutions has also been studied. The unit cell parameters determined from the X-ray diffraction patterns of the sintered samples, and the data obtained from X-ray absorption (XANES and EXAFS) were used to provide information on the environment of Ti atoms. The electrical conductivity of the Ti-YTZP tetragonal solid solutions decreases with increasing titania concentration. EXAFS and XANES results show that as the TiO_2 dissolves into the tetragonal zirconia YTZP matrix, a displacement of Ti^{4+} ions from the center of symmetry seems to take place which leads to a state of non-random substitution of Ti^{4+} ions on Zr^{4+} lattice sites. Ti–O bond distances derived from EXAFS indicate that Ti ions can be in a square-pyramidal arrangememt, i.e. five-fold oxygen coordinated. As consequence, two kinds of cation–oxygen vacancy associations with different diffusion dynamics are created. This results in a decrease in the global concentration of moving oxygen vacancies and, therefore, in a decreasing of the ionic conductivity.

Keywords: C. Electrical properties; Structure; Ti-YTPZ

1. Introduction

Ceramic oxides exhibiting both oxygen ionic and electronic conductivity are widely known as mixed-conductors, and are attracting interest as candidates to be used as electrodes (mainly as anodes) in several applications, as for example in solid oxide fuel cells, oxygen separation membranes and electrocatalysts for the partial oxidation of hydrocarbons [1–3]. The advantages of such mixed-conductors against the purely electronic ceramic electrodes, as for example $La_{1-x}Sr_xMnO_3$ perovskites, are the following: (i) a higher phase stability because of its solid state compatibility with the electrolyte, (ii) the charge-transfer reactions in electronic conductors are limited to regions of three-phase (gas–electrode–electrolyte) contact, while in the mixed-conductors such reactions can take place over the entire electrode–gas interfacial area, and (iii) the above two characteristics lead to a better behavior in that concerning the polarization and efficiency losses at the SOFC operating conditions. Given that an increased electrode polarization is more significant than an increased electrolyte resistance in lowering the SOFC operating temperatures, many efforts are addressed in developing new materials having the adequate level of both ionic and electronic conductivity to enhance the electrode kinetics at lower temperatures [4,5].

A good mixed-conductor ceramic material was prepared in the system ZrO_2–Y_2O_3–CeO_2 [6], but a reasonably good mixed-conductivity was only obtained at temperatures as high as 1500°C, well above the operating temperatures of a SOFC device. In the last decade research efforts have been concentrated mainly in the ZrO_2–Y_2O_3–TiO_2 system and several papers have been published on the characteristics of mixed-conductors of the yttria-stabilized zirconia doped with titania formulated in the cubic zirconia solid solution field of the ternary system. The major paper was that of Liou and Worrell [7] who reported an increase in the electrical conductivity with increasing titania concentration (1–5

* Corresponding author.

0272-8842/99/$ - see front matter
PII: S0272-8842(98)00078-9

mol%), and such increased conductivity was attributed to an enhanced grain boundary one. Contrarily to these results, Naito and Arashi [8] reported that the electrical conductivity of YSZ doped with 0–10 mol% TiO_2 decreased with increasing titania concentration and such a behavior was attributed to the blocking of oxygen ion transport by Ti^{4+} ions in the grain boundary. In the same way Traqueia et al. [9] found that the ionic conductivity of the same titania-doped YSZ decreases with increasing titania content, about one order of magnitude with respect to undoped YSZ, thus confirming the Naito and Arashi [8] results. The role of grain boundaries on the electrical behavior of YSZ-10TiO_2 was also studied by Colomer et al. [10].

Although the titania-doped ZrO_2–Y_2O_3 solid solution with fluorite structure has been quite well studied, the same cannot be said with respect to the titania-doped ZrO_2–Y_2O_3 solid solution with tetragonal structure, and only a few papers have appeared in the literature [11,12]. For example, Kopp et al. [11] studied the stability range of the tetragonal phase in the ZrO_2–Y_2O_3–TiO_2 system and the electrical behavior of titania (1–30 mol%)-doped tetragonal zirconia (1–4 mol% Y_2O_3) compositions was also reported. It was found that the ionic conductivity decreases with increasing TiO_2 content in the 500–700°C temperature range and 10^2 to 10^5 Pa of oxygen partial pressures. Recently Rog and Borchardt [12] reported that the electrical conductivity of tetragonal zirconia (2 mol% Y_2O_3) increased with TiO_2 content (4–13 mol%) in the temperature range 800–1000°C at oxygen partial pressure of 0.1 Pa. A clear explanation for such a contradictory electrical behavior of TiO_2-doped tetragonal zirconia was not reported.

In the present work making use of XRD, SEM, X-ray absorption spectroscopy (XAS) using synchrotron radiation, and particularly the X-ray absorption near-edge fine structure (XANES) and the extended X-ray absorption fine structure (EXAFS) spectra, and the a.c. complex impedance spectroscopic electrical conductivity measurements in air, we try to achieve a better understanding of the role of titania on the ionic conductivity of yttria-doped tetragonal zirconia.

2. Experimental procedure

Yttria-doped tetragonal zirconia, Y-TZP, powders (3 mol% Y_2O_3 from Tosoh Co.) with TiO_2 content ranging from 0 to 20 mol% were prepared by precipitation, on an aqueous suspension of the Y-TZP powders, the appropriate amount of titanium tetrabutoxide with ammonium hydroxide. The final pH of the suspension was $\geq$9 to ensure a qualitative titanium hydroxide precipitation. A homogeneous powder of Y-TZP spheres coated by the titanium hydroxide nanoparticles was obtained at the end of the precipitation process. After being dried at 120°C in air overnight the powders were ball-milled in methanol for 2 h, re-dried at 80°C for 5 h, and calcined at 900°C for 2 h. After calcining the powders were ground and isopressed at 200 MPa and sintered at 1300–1450°C for 5h in air. The crystal structures of the sintered samples were studied using an X-ray diffractometer (Siemens D-5000), measuring the variation of the lattice parameters a and c with increasing titania content. The sintering density of all samples was higher than 96% of theoretical, and the grain size varied from 0.3 to 2 μm in those samples containing the tetragonal zirconia solid solutions as the only phase.

X-ray absorption measurements at the Ti–K edge were made at the storage ring (DCI D44 station) at the LURE synchrotron in Orsay (France) under the operating conditions of 1.85 GeV electron energy and 250 mA ring current. Energy selection was accomplished by using a double crystal monochromator with Si(111) crystals. At the Ti–K absorption edge, a flux of monochromatic synchrotron radiation of 10^{10} photon/s with an energy resolution of about 1.0 eV was obtained.

In the specific case of the TiO_2-YTZP samples, the required amounts of TiO_2-YTZP powders were diluted with boron nitride powder and pressed into an aluminium sample cell with X-ray transparent windows. The XAS spectra were collected at liquid-nitrogen temperature in the transmission mode and using two gas ionization chambers as detectors. The XAS spectra were taken at the Ti–K absorption edge within the energy range between 4900 and 5700 eV with a step width of 0.5 eV. A Ti foil standard (4964.5 eV) was used for energy calibration.

For analysis of the XANES region, the spectra were normalized as previously described [13] avoiding, where possible, deviations between the data and tabulated X-ray absorption coefficients both below and above the edge.

Given that reliable quantitative XANES calculations have only been possible on solids with simple structures, the interpretation of geometrical and chemical changes in more complex structures, as is the present case of TiO_2–Y_2O_3–ZrO_2 solid solutions, will be limited to a qualitative study of these compounds and comparing them with other well-known samples as a reference. On the other hand, since the phase equilibrium diagram of Fig. 3 is tentative, the subsequent XAS studies were carried out only on those samples which appeared to contain the tetragonal zirconia solid solution as the only phase according to XRD. Thus the features of Ti–K XANES for TiO_2-YTZP fine powders containing 5 and 10 mol% TiO_2 were used as ''fingerprints'' to analyze the structural changes, if any, produced as a consequence of the solid solution of TiO_2 into yttria-doped tetragonal zirconia.

The EXAFS spectra were analyzed using the standard EXAFS plane wave equation:

$$\chi(k) = \sum_j \frac{N_j}{kR_j^2} F_j(k) \exp(-2\sigma_j^2 k^2) \exp(-2R_j/\lambda) \sin[2kR_j + \phi_j(k)] \quad (1)$$

where k is the momentum of the photoelectron ejected in the X-ray absorption process, and χ is the normalized oscillations of the fine structure. All the structural parameters contained in this equation as well as their interdependence have been widely described in the literature [14,15] and will not be repeated here. However, it must be mentioned that the EXAFS spectra were analyzed taking into account the PC program developed by Bonin et al. [16] using the theoretical amplitude and phases shift function proposed by Rehr et al. [17]. In this way the coordination numbers (N_j), the bond distance (R), and the relative bond length disgregacion or Debye–Waller factor ($\Delta\sigma^2$) with reference to the model compound were obtained. To take as an example in this study Fourier transforms (FTs) of Ti EXAFS from $K=2$ to 12 Å^{-1} were back-transformed from $R=1$ to 2.1 Å to obtain the Ti–O first shell and $R=2$ to 3 Å for the Ti–Ti second shell. These FTs give pseudo-radial distribution functions around the absorber cations, and curve fitting, as mentioned above, utilized the theoretical amplitude and phase shift functions calculated from the FEFF program [17]. For Ti EXAFS, empirical amplitude and phase functions derived from TiO_2 were used to fit the Ti–O shells, with Fourier filter windows of 0.9–1.8 Å.

Platinum paste (Engelhard 6082) was painted on both sides of the sintered discs which were dried in an oven at 120°C to eliminate the solvent. After drying, the electrode samples were annealed at 800°C for a short time, about 30 min, to avoid an excessive shrinkage of the platinum electrodes. To these electrode samples were welded platinum lead wire and placed in the hot zone of a programmed furnace with a chrome–alumel thermocouple located on the mid-point of the electrode sample.

The temperature dependence of electrical conductivity measurements were carried out using an impedance analyzer (Hewler Packard model 4192A) in the frequency range of 5 Hz to 13 MHz. Measurements were made in air in the temperature range 200–800°C. For comparison, an undoped Y-TZP sample sintered in the same conditions as for TiO_2-doped Y-TZP ones was used.

3. Experimental results

3.1. Tetragonal phase Ti-YTZP existence field

As can be seem in Fig. 1 the lattice parameters a and c of tetragonal zirconia Y-TZP decrease and increase, respectively, with increasing TiO_2 concentration and appear to reach a constant at about 13 mol% TiO_2. Fig. 1

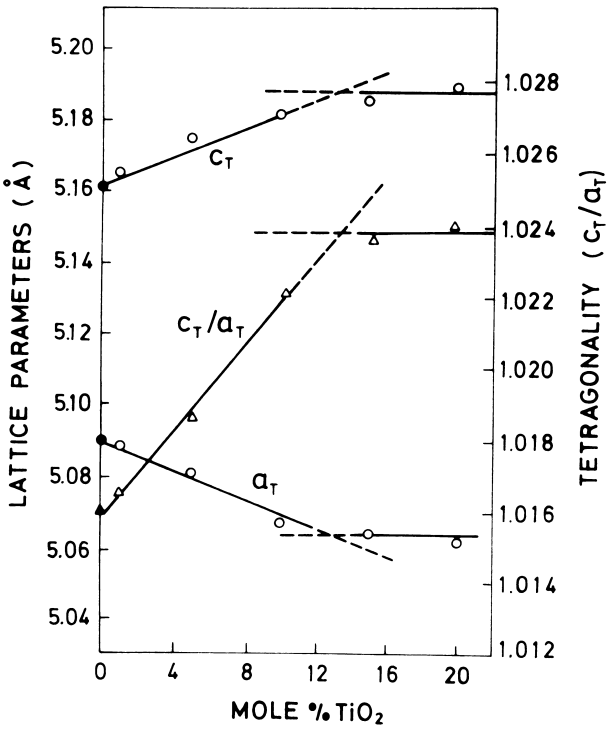

Fig. 1. Variation of unit-cell dimensions and tetragonality of TiO_2-doped Y-TZP solid solutions after sintering at 1450°C.

also shows the variation of the tetragonality c_t/a_t as a function of the TiO_2 content. As mentioned above, the tetragonality remains constant beyond 12 mol% TiO_2, confirming the statement for the solubility limit for TiO_2 in tetragonal zirconia Y-TZP. These results are consistent with the SEM observations, as shown in Fig. 2, in which a composition containing 15 mol% TiO_2 showed both a considerable amount of a second phase, the zirconium titanate (ZT), and an enhanced grain growth. Therefore, the solubility limit of TiO_2 into tetragonal zirconia Y-TZP is well below 15 mol% up to 1450°C. These solid solubility data for TiO_2 in Y-TZP are somewhat lower than those reported by Lin et al. [18] and Kontouros et al. [19], but they are in agreement with Hoffman et al. [20] and Rog and Borchardt [12]. The different powder preparation methods used could be the main source for the controversy.

In order to establish the tetragonal zirconia solid solution field in the ZrO_2–TiO_2–Y_2O_3 system, a series of solid-state reactions between tetragonal zirconia ZrO_2–$15TiO_2 + Y_2O_3$ and Y-TZP + TiO_2, not shown here, were studied at 1450°C [21]. Occasionally, a composition containing 90 mol% (ZrO_2–8 mol% Y_2O_3)–10 mol% TiO_2 (YSZ-10Ti) also was sintered in the same conditions. From the results obtained a tentative phase equilibrium diagram at the ZrO_2 corner of the ternary system is proposed as shown in Fig. 3, which is somewhat different to that previously established by Tsukuma [22] and Kontouros et al. [19].

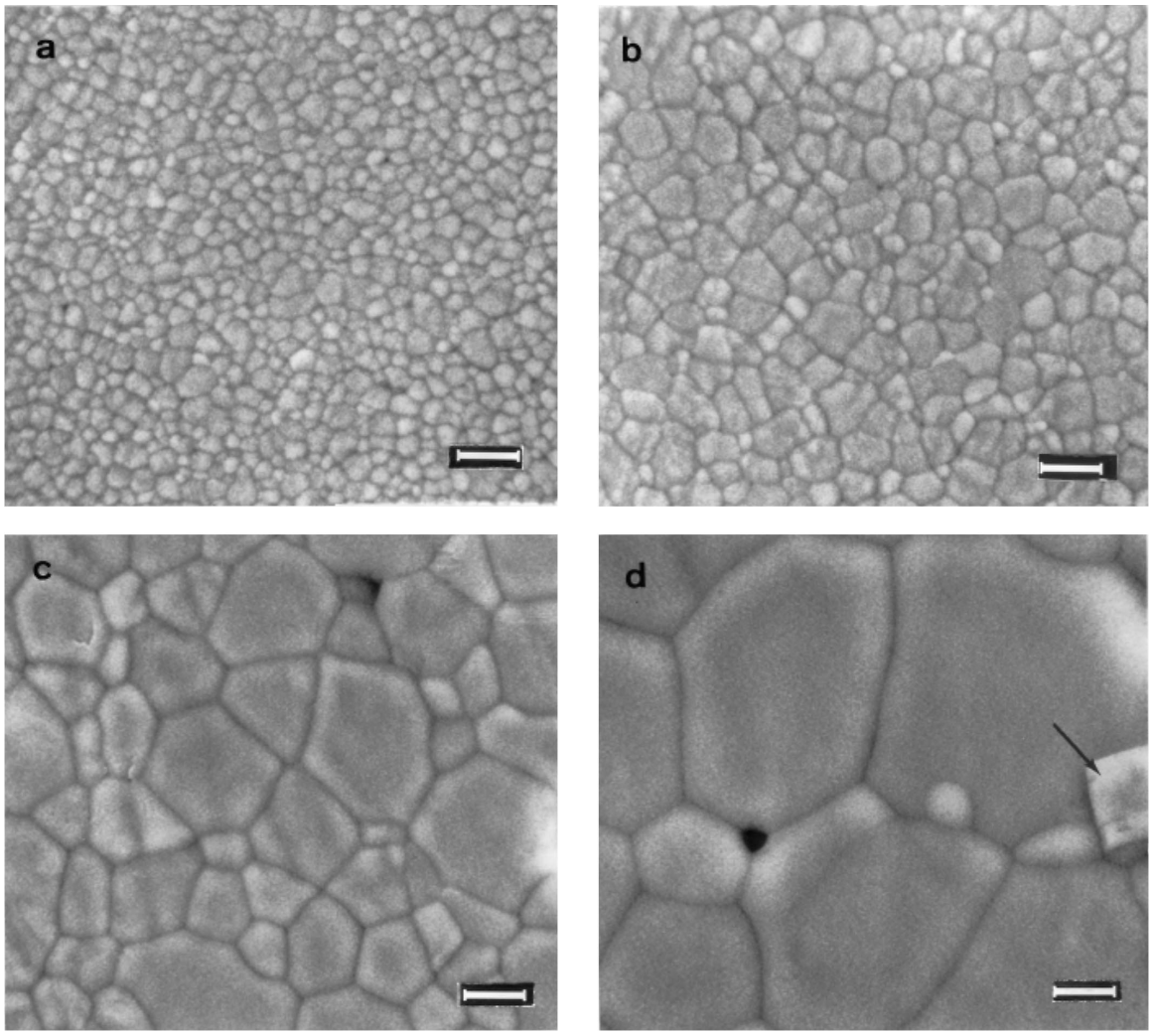

Fig. 2. SEM micrographs of surfaces of as sintered TiO_2-YTZP samples at 1450°C: (a) 1 mol% TiO_2, (b) 5 mol% TiO_2, (c) 10 mol% TiO_2 and (d) 15 mol% TiO_2. Arrow indicates second phase. Bar = 2 μm.

3.2. EXAFS spectra at the Ti–K edge

The room temperature Ti–K-edge EXAFS spectra of the two 5Ti-YTZP and 10Ti-YTZP tetragonal zirconia solid solutions are shown in Fig. 4(a). As mentioned before, the energy zero was taken as the K-edge energy of pure Ti metal (4966.4 eV). The normalized Ti EXAFS for those tetragonal zirconia solid solutions plotted as $\chi(k)$ are shown in Fig. 4(b), and the Fourier transformation of these radial structure peak yields a filtered $\chi(k)$ signal, as shown in Fig. 4(d), which were used to study the local structure around titaniun cations.

Utilizing amplitude and phase shift functions derived from the TiO_2 model system a quantitative analysis of the first Ti–O shell, as shown in Fig. 4(c), was performed. The first mayor peak in the FTs, between about 1.3 and 2 Å, corresponds to the nearest neighbor around the Ti cation and the second peak, between 2 and 3 Å, corresponds to the next nearest neighbors, i.e. Ti–Ti or Ti–Zr cations. The peaks for higher R values belong to outer cation–cation shell. From the FTs a slight decreasing of the amplitude of Ti EXAFS with increasing TiO_2 content can be noticed, which is in close agreement with the results obtained for Ce-doped tetragonal zirconia [23], and indicates an increased distortion of the cation network.

Quantitative fitting results, as is shown in Table 1, for the Ti–O shell led to two sets of bond lengths, 1.73 and 1.87 Å for the 5Ti-YTZP solid solution, and a total coordination number of ~6. In the same way, two sets of bond lengths, 1.88 and 2.05 Å with a total coordination number of ~4, were found for the 10Ti-YTZP solid solution. Thus, the local environment around Ti^{4+} seems to be concentration-dependent [24]. Therefore these results are consistent with a change of coordination number (6 to 5 or 4 for Ti) from pure TiO_2 to tetragonal zirconia solid solutions. Finally, quantitative

fitting of the first Ti-cation (Zr and/or Ti) shell were performed using calculated amplitude and phase functions of a Ti–Ti pair. A distance of 2.81 Å was obtained in the specific case of the 10Ti-YTZP tetragonal zirconia solid solution. No quantitative analysis was performed for the 5Ti-YTZP one. That Ti–Ti distance is much shorter than that of the corresponding Zr-cation shell (3.61–3.62 Å) [25]. This can indicate that Ti^{4+} ions do not randomly substitute Zr^{4+} lattice sites according to a statistical process [26].

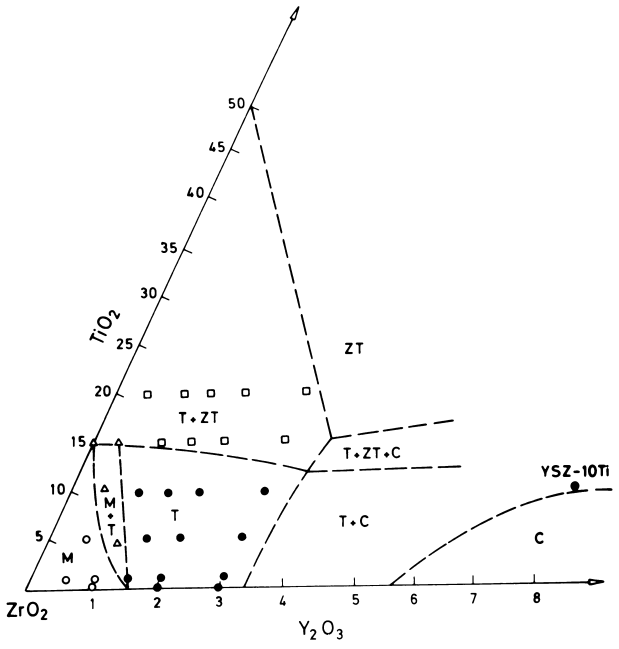

Fig. 3. Room temperature phase composition at the ZrO_2-rich region of the ZrO_2–Y_2O_3–TiO_2 system after sintering at 1450°C.

3.3. XANES spectra

X-ray absorption near-edge (XANES) spectra at the Ti–K absorption edge for 5Ti-YTZP and 10Ti-YTZP are shown in Fig. 5. Given that the structure of both samples is tetragonal the spectra are quite similar. The energy of the Ti–K absorption edge corresponds to the electronic transition from the 1s core level to unoccupied high-energy states, and has been determined as the inflexion point of rising edge of the XAS data. Such a shoulder was located at about 4972.8 eV which is somewhat higher than that of metallic Ti as consequence of the different oxidation state of that cation in both cases. For energies lower than that of the Ti–K absorption edge a relatively sharp pre-peak located at almost the same energy (4967.5 eV), but with different intensity for 5 Ti-YTZP and 10Ti-YTZP samples, was present in the XANES spectra. Above the Ti–K absorption edge the XANES spectra display a prominent

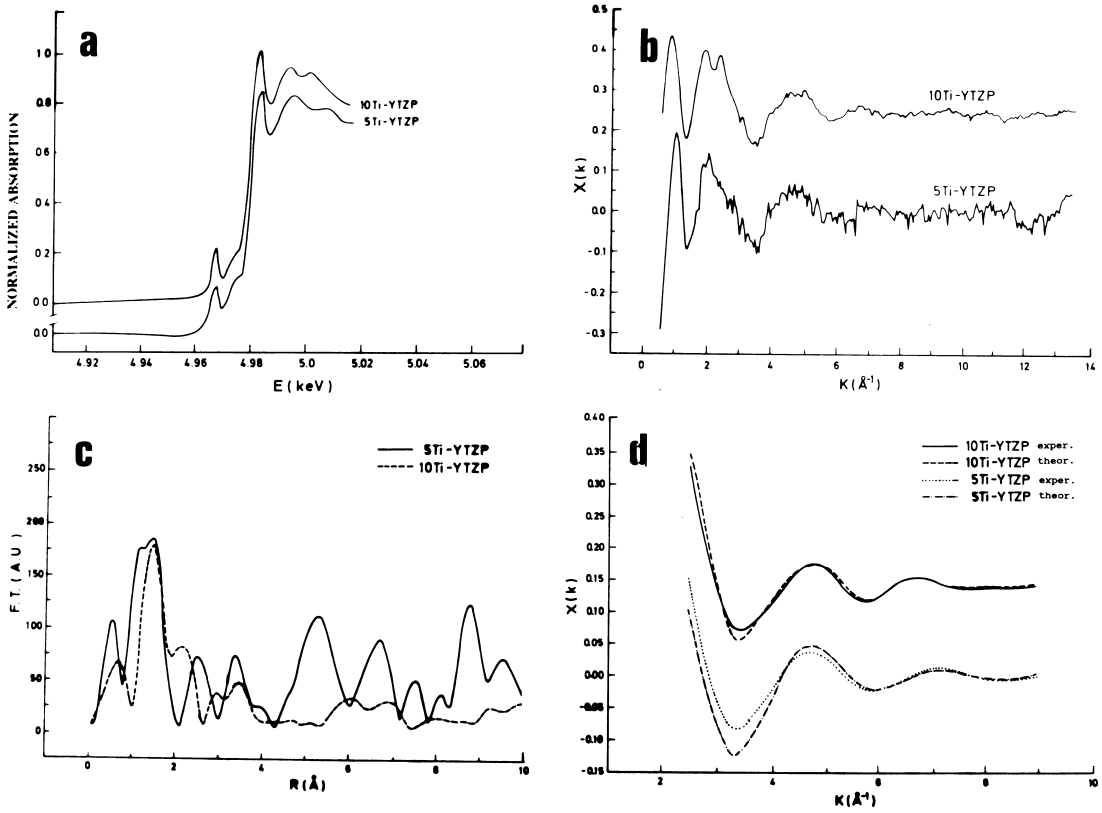

Fig. 4. X-ray absorption of 5Ti-YTZP and 10Ti-YTZP tetragonal zirconia solid solutions at the Ti–K edge: (a) XANES, (b) normalised EXAFS $\chi(k)$, (c) Fourier transform, and (d) inverse transform of (c).

peak located at slightly different energies, 4983.6 and 4983.2 eV, for 5Ti-YTZP and 10Ti-YTZP samples, respectively.

Given that the XANES spectra can be taken as the fingerprints to be compared with those of well-known structure compounds as reference, then the XANES spectra of our tetragonal zirconia solid solutions were compared with those, not shown here, of the rutile (with Ti ions six-fold coordinated), $Ti(OEt)_4$ (five-fold coordinated), and Ba_2TiO_4 and $Ti(OAm)_4$ (four-fold coordinated), respectively [27–30]. The octahedral coordinated compounds (rutile and/or anatase) are characterized by several pre-edge peaks of low intensity and centered at an energy of 4968 eV, Ba_2TiO_4 and $Ti(OAm)_4$ with Ti ions tetrahedral coordinated exhibited a strong pre-edge peak at an energy of 4967 eV, $Ti(OEt)_4$ with Ti ions coordinated by five oxygen ions in a square-pyramidal distribution showed a relatively sharp pre-edge peak at 4967.5 eV. Then, from the above XANES spectra data it seems reasonable to state that the intensity, shape and energy position (4967.5 eV) of the pre-edge peak of the Ti-YTZP tetragonal zirconia solid solutions compares well with that of the $Ti(OEt)_4$ compounds with a square-pyramidal arrangement.

The characteristics of the post-edge peak present in the Ti-YTZP XANES spectra, i.e. lower energy and higher intensity for increasing TiO_2 content, can indicate a change in the geometrical arrangement of the scatterer ions in the Ti environment. Such a suggestion is consistent with the results of Zschech et al. [26].

Table 1
Fitting results of Ti EXAFS for Ti-doped tetragonal zirconia samples

	M–O	R (Å)	CN	$\Delta\sigma^2$ (Å$^2\times10^{-3}$)
First shell				
5Ti-YTZP	Ti–O	1.73	2.6	0.1
	Ti–O	1.87	3.8	0.1
10Ti-YTZP	Ti–O	1.88	2.2	0.1
	Ti–O	2.05	1.6	0.1
Second shell				
10Ti-YTZP	Ti–Ti	2.81	2.2	0.1

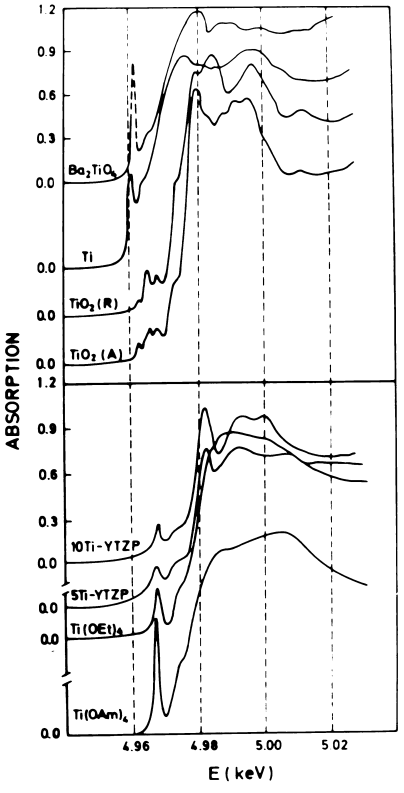

Fig. 5. Comparison plot of K-edge XANES spectra of Ti in 5Ti-YTZP and 10Ti-YTZP tetragonal zirconia solid solutions with several Ti–O reference compounds.

3.4. Electrical properties

The a.c. conductivity results were plotted in the complex impedance plane, and a typical a.c. impedance spectrum for titania-doped tetragonal zirconia (5Ti-YTZP) at 449°C is shown in Fig. 6. As can be seen, three well-developed semicircles can be distinguished which are related to the bulk, grain boundary, and electrode relaxation phenomena at high, intermediate, and low frequencies, respectively [31]. From the intersection of the first semicircle at the higher frequency with the real axis the bulk resistance can be obtained. In the same way the sum of bulk and grain boundary resistances was calculated from the second one. From the intersection of the third one, the sum of bulk, grain boundary and electrode resistances can be estimated. The specific total conductivity (σ_t) can be easily calculated taking into account the platinum electrode area (A) on either side of the sample, and the length (L) between the two platinum electrodes. For example, the bulk conductivity (σ_b) was calculated using the following known equation [32]:

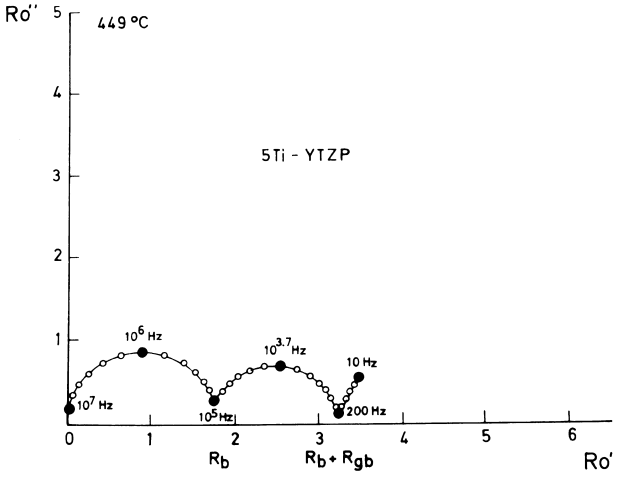

Fig. 6. Complex impedance plots for 5Ti-YTZP at 449°C in air.

$$\sigma_b = \frac{1}{R_b}\frac{L}{A} \quad (2)$$

where R_b is the intersection of the first semicircle as indicated in Fig. 6. A quite similar a.c. impedance spectrum was obtained for the 10Ti-YTZP sample. It must be mentioned that poorly developed grain boundary semicircles were obtained with increasing temperature in both titania-doped YTZP samples, and it becomes difficult to analyze the impedance data in terms of bulk and grain boundary contributions. However, in order to know what is the predominant conduction mechanism, an attempt to calculate the bulk and grain boundary conductivities at that temperature range in which the two first semicircles were quite well developed, was made. With these conductivity data and assuming that the electrical conductivity σ follows an Arrenius equation of the type:

$$\sigma = \sigma_o \exp(-E_a/RT) \quad (3)$$

where T is the absolute temperature, σ_o is a constant, E_a is the activation energy for the motion of charges, and R is the gas constant, the temperature dependence of the bulk, grain boundary, and total conductivities for 5Ti-YTZP, 10Ti-YTZP, and undoped Y-TZP samples was studied. In Table 2 the activation energy values for the three samples in the temperature range 300–700°C are shown.

From the Arrhenius plot a general trend to decrease the electrical conductivity with increasing titania content as shown in Fig. 7, can be observed, and from Table 2 the similar activation energy value for the bulk and the total conductivity processes allows one to assume that a bulk oxygen ion transport seems to be predominant in the samples studied.

4. Discussion

From the XRD results, and SEM observations (see Figs. 1 and 2) it can be stated that the solubility limit for titania in tetragonal zirconia (3 mol% Y_2O_3) up to 1450°C is close to ~12 mol%. Compositions containing higher titania content showed the incipient presence of a second phase, the zirconium titanate (ZT), and for higher yttria content appeared the zirconia phase with cubic structure in agreement with that established for the ZrO_2–Y_2O_3 binary system [33,34]. Above 1450°C, the amount of zirconium titanate strongly increased.

Table 2
Activation energy values (eV) of the conductivity

Sample	σ_b	σ_{gb}	σ_t
YTZP	0.86	1.01	0.90
5Ti-YTZP	0.97	1.17	1.04
10Ti-YTZP	1.02	1.16	1.04

It was also noticed that the tetragonality, c/a, of the zirconia solid solutions increases with increasing content of the TiO_2 dopant [21], and this became constant for a TiO_2 content near to 14 mol% confirming the above statement for the solubility limit of TiO_2 in tetragonal zirconia, Y-TZP, 3 mol% Y_2O_3, in close agreement with the results of Lin et al. [18]. This solid solution with a tetragonality of about 1.024, much higher than that of the binary tetragonal zirconia–yttria solid solution [34], 1.016, is also stable at room temperature. Albeit the stability of the tetragonal zirconia solid solution needs the creation of oxygen vacancies, and the addition of Ti^{4+} implies a dilution effect with a slight decreasing of the oxygen vacancy concentration, then the enhanced stability of the ternary tetragonal zirconia solid solutions can be explained by two coadjutant effects: (i) the presence of a relatively high concentration of oxygen vacancies introduced by Y^{3+} dopant and (ii) albeit the Ti dopant could decrease the stability of the Y-stabilized tetragonal zirconia by diluting the effect of the oxygen vacancies introduced by Y^{3+} but the measured Ti–O distances (1.88 Å), being shorter than the Zr–O_I distances (2.10Å), leads to an accentuated bonding anisotropy of the layer-like zirconia structure and, therefore, to a higher tetragonality. Besides this the size of the Ti^{4+} cation ($RTi^{4+} = 0.745$ Å) is much smaller than Zr^{4+} ($RZr^{4+} = 0.86$ Å), adopting a five-fold coordination would favor a packing in the form of a relatively ordered layer-like structure, thus alleviating the oxygen overcrowding around Zr cations similarly to that which occurs in the GeO_2-doped tetragonal zirconia [23,35].

Ordering involving the smallest Ti cations was not demonstrated in the case of the titania-doped YTZP solid solutions, but a Ti cationic short-range ordering was detected by TEM in the ZrO_2–CeO_2–TiO_2 system

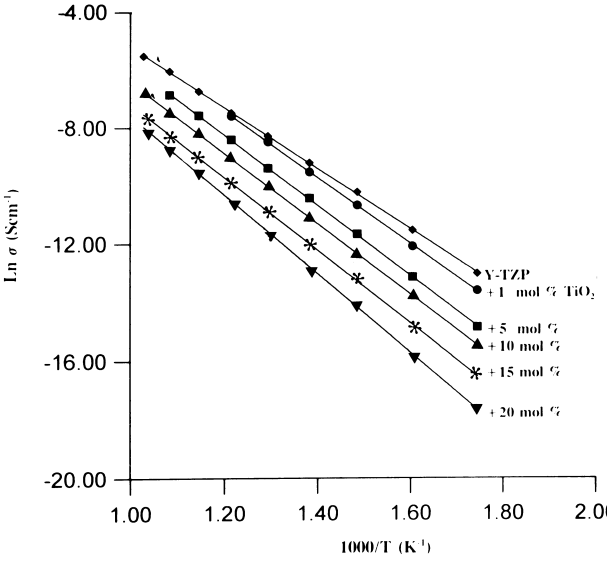

Fig. 7. Temperature dependence of the total conductivity in $(TiO_2)_x$–$(3Y\text{-}TZP)_{1-x}$ tetragonal zirconia solid solutions.

for a stable composition having a tetragonality as high as 1.032 [36]. The measured Ti–Ti distances (2.81 Å) shorter than 3.62 Å for Zr–Zr ones, allows us to assume a certain Ti cationic ordering sufficient to reduce the strain energy of the tetragonal lattice leading to a higher stability of the titania-doped tetragonal zirconia solid solutions.

Fourier transforms (FTs) of the Ti EXAFS for tetragonal 5Ti-YTZP and 10Ti-YTZP, as pseudo-radial distribution functions of the absorber atom, can be used to compare structures surrounding the Ti cation (see Fig. 4). From those results, combined with those obtained from the XANES spectra (see Fig. 5), it can be stated a non-random substitutional model when dissolving TiO_2 into yttria-doped tetragonal zirconia. The ternary Ti-YTZP solid solution becomes more distorted with increasing TiO_2 content. Such an increasing distortion indicates a change in the coordination number of the Ti cations with the subsequent loss of centrosymmetry in the crystal lattice of the tetragonal zirconia. Such a statement is supported by the increase of the intensity of the pre-edge peak and the decrease in energy of the post-edge peak with increasing TiO_2 content, as shown in the XANES spectra (Fig. 5).

From the EXAFS spectra analysis for the 5Ti-YTZP sample it can be noticed the Ti–O distance is 1.73 Å, which is comparable to that corresponding to Ti^{4+} cations tetrahedrally coordinated as in the case of the compounds Ba_2TiO_4 (1.74 Å) and $Ti(OAm)_4$ (1.81 Å), but the total coordination number for the 5Ti-YTZP sample was near to 6. This result leads one to assume that, similarly to that occurring in TiO_2–SiO_2 glasses [29], when the TiO_2 concentration was low the Ti^{4+} prefers the octahedral coordination in the glass network, and for higher concentration the Ti^{4+} adopts the five-fold coordination. A similar phenomenon seems to be present in the Ti-YTZP solid solutions with increasing TiO_2 content. Such a coordination change leads one to assume a strong distortion of the tetragonal zirconia lattice, albeit the measured Debye–Waller factors (see Table 1) being positive, are relatively small to support a very severe tetragonal zirconia lattice distortion. Therefore with the present EXAFS and XANES data it can be said that the Ti^{4+} cations in the Ti-YTZP solid solutions are displaced from the center of the coordination polyhedron adopting a non-octahedral coordination, presumably five-fold coordinated in a square-pyramidal arrangement. In our opinion, an exhaustive study of these Ti-YTZP ternary solid solutions which includes the EXAFS spectra at the Zr–K and Y–K edges would contribute to a better knowledge of the crystal chemistry of Ti^{4+} in these zirconia solid solutions. Such work is now in progress.

Finally, the shorter Ti–O distances favoring a movement to an off-center position, and the Ti–Ti measured distances lead one to assume a strong interaction between the Ti cations with a certain tendency to the formation of clusters. Such a clustering phenomenon can provoke a different oxygen ion bonding in the tetragonal zirconia lattice and, of course, a different bond strength of the oxygen vacancies associated with both Zr or Ti cations with different coordination numbers.

The electrical behavior of TiO_2-doped zirconia solid solutions has been widely studied mainly in the cubic structure. However, there is no coincidence in the results of different authors, thus while for Liou and Worrel [7] the electrical conductivity in air of TiO_2-doped cubic zirconia increases with increasing TiO_2 content, for Naito and Arashi [8] the results are contrary. From the complex impedance electrical measurements both supported their conclusions on the basis of an enhancement of the grain boundary conductivity by the presence of small amounts of impurities segregated at the grain boundary [7], or the conductivity decrease was due to a blocking effect of the Ti^{4+} ions located at the grain boundaries on the oxygen ion transport [8]. The first idea was also supported by Matsui [37]. None of these studies explained the true role of the crystal chemistry of the Ti ions in the TiO_2–cubic zirconia solid solutions. Recently Traqueia et al. [9], making use of Raman spectroscopy, tried to correlate the electrical conductivity decrease with increasing titania content in TiO_2-doped cubic zirconia with the presence of a tetragonal short-range order in the cubic zirconia matrix. Such a short-range order decreased the concentration of the mobile oxygen vacancies and, thus, the electrical conductivity also was decreased.

The present results on the electrical conductivity in air of TiO_2-doped tetragonal zirconia solid solutions show the same dependence, i.e. the electrical conductivity in air decreases with increasing titania content. Such a behavior is explained on the basis of the study of the Ti ions' local environment from the EXAFS and XANES spectra data (see Figs. 4 and 5). From those results and taking into account the model of Li et al. [13], it is assumed that Y^{3+} cations substitutes for Zr^{4+} in the cation network adopting a YO_8 structure and, therefore, Y^{3+} will not be associated with oxygen vacancies. This being so, this eight-fold dopant coordination leaves oxygen vacancies next to both Zr and Ti cations, since the Zr(Ti)-vacancy pairing is energetically more favorable than Y-vacancy pairing in Y-doped zirconia as previously suggested [13]. In that situation, undersized tetravalent dopants, such as Ti^{4+}, which do not substitute randomly for Zr ions in tetragonal zirconia solid solutions and adopting a five-fold coordination with a square-based pyramidal arrangement, are thus in competition with Zr ions for the oxygen vacancies. On that basis, two kinds of vacancy (V_o)–cation associations have to be formed, one of them being Zr–V_o–Zr in which the oxygen vacancy is associated to a cation octahedrally coordinated, and the other one

being Ti–V_o–Ti with the oxygen vacancy associated to a cation five-fold coordinated. With such a statement it must be also assumed two oxygen sublattice with different vacancy diffusion dynamics. Given that the Ti–O distances are shorter that the Zr–O ones, we state that the oxygen vacancy diffusion on the octahedrally coordinated sublattice is more rapid than on the square-based pyramidal five-fold sublattice, and a hindering of the mobility of the oxygen vacancies is produced, thus, by the presence of the Ti ions in the TiO_2-doped tetragonal zirconia solid solutions. This is supported by the fact that the activation energy for the conduction process is higher in TiO_2-doped YTZP than in undoped-YTZP (see Table 2). On the other hand, the shorter Ti–Ti measured distances will show a certain tendency to the formation of Ti clusters, and thus to an increasing degree of the oxygen vacancy–titanium cation complex associations. The different activation energies for the oxygen ion transport in TiO_2-doped YTZP and undoped-YTZP solid solutions can be a result of both the lower oxygen vacancy concentrations (the dilution effect of the Ti^{4+} ions), and the different coulombic attractions between the two tetravalent cations Zr^{4+} and Ti^{4+}, with different coordination numbers, and an oxygen vacancy.

5. Summary and conclusions

From the XRD lattice parameter measurements on $(TiO_2)_x$–(Y-TZP)$_{1-x}$ ($x = 1$–20 mol%) samples sintered in the temperature range 1300–1450°C, the ZrO_2-rich region of the ZrO_2–Y_2O_3–TiO_2 ternary system has been established. Titania can completely dissolve in stabilized tetragonal zirconia (3 mol% Y_2O_3) up to about 12–14 mol%, forming room temperature stable ternary tetragonal zirconia solid solutions. The lattice parameters a_t and c_t of these ternary solid solutions decreases and increases, respectively, with titania content and, in spite of the strong increasing of the tetragonality c_t/a_t, the tetragonal structure as single phase was retained for TiO_2 concentrations lower than 15 mol%.

The X-ray absorption studies (XANES) lead one to state that, as the TiO_2 is dissolved, a certain distortion of the Ti cation coordination and a loss of centrosymetry in the Ti-YTZP tetragonal zirconia crystal lattice takes place. In that way, we propose that Ti^{4+} ions do not form a random substitutional solid solution with Zr^{4+} ions. From the EXAFS spectra, the measured Ti–O distances which are much shorter than the main Zr–O_I ones, lead one also to assume a stronger Ti–O bond strength giving rise to an increase in the anisotropy of the tetragonal layer structure and in its tetragonality. On the other hand, the small Ti^{4+} ion radius and the measured Ti–Ti distances allow us to assume a strong interaction between the Ti ions in the Ti-YTZP solid solutions leading to the formation of Ti ion clusters. Given that the vacancies introduced by the oversized dopant (Y^{3+}) are located as nearest neighbors to Zr^{4+} ions, then undersized tetravalent dopant (Ti^{4+}) competes with Zr^{4+} ions for the oxygen vacancies in zirconia solid solutions. On that basis, it is believed that two kinds of oxygen vacancy–cation associations, Zr–Vö–Zr and Ti–Vö–Ti, exist in the zirconia lattice.

The incorporation of titania into yttria-stabilized tetragonal zirconia decreases the ionic conductivity of the formed ternary tetragonal zirconia solid solutions with increasing titania content. From the EXAFS results, it is believed that such a conductivity decrease is due to the existence of the above-mentioned two oxygen vacancy–cation associations in the zirconia lattice, Vö–Ti five-fold coordinated and Vö–Zr octahedrally coordinated with different vacancy diffusion dynamics Vö–Zr$\gg$Vö–Ti, resulting in a decreasing in the global concentration of moving oxygen vacancies and, thus, in a decreasing of the ionic conductivity. Besides this, the tendency of the small Ti^{4+} cations to form clusters will give rise to the formation of more complex –Ti–Vö–Ti–Vö– associations which also will hinder the mobility of the oxygen vacancies during the conduction process.

Acknowledgements

This work was supported by the Spanish Commission of Science and Technology under contract MAT 97-O679-C02-01.

References

[1] P. Han, W.L. Worrell, Mixed (oxygen ion and p-type) conductivity in yttria-stabilized zirconia containing terbia, J. Electrochem. Soc. 142 (1995) 4235–4246.
[2] A.J. Burggraaf, B.A. Boukamp, I.C. Vinke, K.J. de Vries, Recent developments in oxygen-ion conducting solid electrolites and electrode materials, in: R.C.A. Catlow (Ed.), Advances in Solid State Chemistry, vol. 1, JAI Press, London, 1989, pp. 259–294.
[3] H.L. Tuller, Mixed conduction in nonstoichiometric oxides, in: O.T. Sorensen (Ed.), Nonstoichiometric Oxides, Materials Science Series, Academic Press, New York, 1981, pp. 271–332.
[4] S. Kramer, M. Spears, H.L. Tuller, Electrical properties of Ti-rich $Gd_2(Zr_xTi_{1-x})_2O_7$, in: T.O. Mason, J.L. Ronbart (Eds.), Point Defects and Related Properties of Ceramics, Ceramic Transactions, vol. 24, American Ceramic Society, Cincinnati, OH, 1991, pp. 203–210.
[5] M. Spears, H.L. Tuller, Electrical conductivity and phase stability of ruthenium substituted gadolinium titanate, in: T.A. Ramanarayanan, W.L. Worrell, H.L. Tuller (Eds.), Ionic and Mixed Conducting Ceramics, Electrochemical Society, Pennington, NJ, 1994, pp. 94–105.
[6] B. Cales, J.F. Baumard, Mixed conduction and defect structure of ZrO_2–CeO_2–Y_2O_3 solid solutions, J. Electrochem. Soc. 131 (1983) 2407–2413.
[7] S.S. Liou, W.L. Worrell, Electrical properties of novel mixed-conducting oxides, Appl. Phys. A 49 (1989) 25–31.
[8] H. Naito, H. Arashi, Electrical properties of ZrO_2–TiO_2–Y_2O_3, Solid State Ionics 53–56 (1992) 436–441.

[9] L.S.M. Traqueia, T. Pagnier, F.M.B. Marques, Structural and electrical characterization of titania-doped YSZ, J. Europ. Ceram. Soc. 17 (1997) 1019–1026.
[10] M.T. Colomer, C.S.M. Traqueia, J.R. Jurado, F.M.B. Marques, Role of grain boundaries on the electrical properties of titania-doped YSZ, Mater. Res. Bull. 30 (1995) 515–522.
[11] A. Kopp, H. Nate, W. Weppner, P. Kontouros, H. Schubert, Ionic and electronic conductivity of TiO_2–Y_2O_3-stabilized tetragonal zirconia polycrystals, in: S.P.S. Badwal, M.J. Bannister, R.H.K. Hannink (Eds.), Science and Technology of Zirconia V, Technomic, Lancaster, PA, 1993, pp. 567–575.
[12] G. Rog, G. Borchardt, Electrochemical properties of ZrO_2–Y_2O_3–TiO_2 ceramics, Ceramics International 22 (1996) 149–154.
[13] P. Li, I.W. Chen, J.A. Penner-Hahn, Effects of dopants on zirconia stabilization—an X-ray absorption study: I. Trivalent dopants, J. Am. Ceram. Soc. 77 (1994) 118–128.
[14] B.K. Teo, EXAFS: Basic Principles and Data Analysis, Springer-Verlag, New York, 1986.
[15] R.A. Scott, Measurement of metal–ligand distances by EXAFS, Methods Enzymol. 177 (1985) 414–459.
[16] D. Bonin, P. Kaiser, C. Fregny, J. Desbarres, Structures fines d'absorption en chimie, in: H. Dexpert, A. Michaloria, M. Verdagluer (Eds.), Orsay, 1989 [Chapter 3].
[17] J.J. Rehr, J.M. de Leon, S.J. Zabinsky, R.C. Albers, Theoretical X-ray absorption fine structure standards, J. Am. Chem. Soc. 113 (1991) 5135–5140.
[18] C.L. Lin, D. Gan, P. Shew, The effects of TiO_2 addition on the microstructure and transformation of ZrO_2 with 3 and 6 mol% Y_2O_3, Mater. Sci. Eng. A129 (1990) 147–155.
[19] P. Kontouros, G. Petzow, Defect chemistry, phase stability and properties of zirconia polycristals, in: S.P.S. Badwal, M.J. Bannister, R.H.K. Hannink (Eds.), Science and Technology of Zirconia V, Technomic, Lancaster, PA, 1993, pp. 30–48.
[20] H. Hoffman, B. Michel, L.J. Gauckler, Zirconia powder for TZP-ceramics Ti–Y-TZP, in: S. Meriani, C. Palmonari (Eds.), Advances in Zirconia Science and Technology—Zirconia '88, Elsevier Applied Science, London, 1989, pp. 119–129.
[21] F. Capel, Ph.D. thesis, University Complutense of Madrid, Spain, 1998.
[22] T. Tsukuma, Transparent titania–zirconia–yttria ceramics, J. Mater. Sci. Lett. 5 (1986) 1143–1144.
[23] P. Li, I.W. Chen, J.E. Penner-Hahn, Effect of dopants on zirconia stabilization—an X-ray absorption study: II. Tetravalent dopants, J. Am. Ceram. Soc. 77 (1994) 1281–1288.
[24] P. Li, I.W. Chen, J.E. Penner-Hahn, X-ray absorption studies of zirconia polymorphs. II. Effect of Y_2O_3 dopant on ZrO_2 structure, Phys. Rev. B 48 (1993) 10074–10081.
[25] R.C. Catlow, A.V. Chadwick, G.N. Greaves, L.M. Moroney, EXAFS study of yttria-stabilized zirconia, J. Am. Ceram. Soc. 69 (1986) 272–277.
[26] E. Zschech, P.N. Kontouros, G. Petzow, P. Behrens, A. Frahm, R. Frahm, Synchrotron radiation Ti–K XANES study of TiO_2–Y_2O_3-stabilized tetragonal zirconia polycrystals, J. Am. Ceram. Soc. 76 (1993) 197–201.
[27] G.A. Waychunas, Synchrotron radiation XANES spectroscopy of Ti in minerals: effects of Ti-bonding distances, Ti valence, and site geometry on absorption edgestructure, Am. Mineral. 72 (1987) 89–101.
[28] T. Dumas, J. Petiau, EXAFS study of titanium and zinc environments during nucleation in a cordierite glass, J. Non-Cryst. Solids 81 (1986) 201–220.
[29] C.A. Yarker, P.A.V. Johnson, A.C. Wright, J. Wong, R.B. Lyle, F.W. Lyle, R.N. Sinclair, Neutron diffraction and EXAFS evidence for TiO_5 units in vitreous $K_2O.TiO_2.2SiO_2$, J. Non-Cryst. Solids 79 (1986) 117–136.
[30] J. Livage, Molecular design of transition metal alkoxide precursors, in: B.I. Lee, E.J.A. Pope (Eds.), Chemical Processing of Ceramics, Marcel-Decker, New York, 1994, pp. 3–57.
[31] M.J. Verkerk, B.J. Middelhuis, A.J. Burggraaf, Solid State Ionics 6 (1982) 159.
[32] J.A. Kilner, B.C.H. Stule, Mass transport in anion-deficient fluorite oxides, in: D.T. Korensen (Ed.), Nonstoichiometric oxides, Academic Press, New York, 1981, pp. 233–269.
[33] C. Pascual, P. Durán, Phase equilibrium and ordering in the ZrO_2–Y_2O_3 system, J. Am. Ceram. Soc. 66 (1983) 23–27.
[34] H.G. Scott, Phase relations in the zirconia–yttria system, J. Mater. Sci. 10 (1975) 1527–1535.
[35] D. Michel, L. Mazerolles, M. Perez-Jorba, Fracture of metastable tetragonal zirconia crystals, J. Mater. Sci. 18 (1983) 2618–2628.
[36] V.C. Pandolfelli, W.M. Rainforth, R. Stevens, Tetragonal zirconia polycrystals in the ZrO_2–TiO_2–CeO_2 system, in: G. de With, R.A. Terpstra, R. Metselaar (Eds.), Proc. 1st European Ceramic Society Conf., Elsevier Science, New York, 1989, pp. 161–165.
[37] N. Matsui, Effects of TiO_2 addition on electrical properties of yttria-stabilized zirconia, Denki Kagaku 58 (1990) 716–722.